(1)

RAMAN HYDROGEN SENSOR
PHASE I FINAL REPORT

SPECTRAL SCIENCES INCORPORATED

111 South Bedford Street, Burlington, Massachusetts 01803 (617) 273-4770

SSI-TR-205

RAMAN HYDROGEN SENSOR
PHASE I FINAL REPORT

S. M. Adler-Golden and J. Lee
Spectral Sciences, Inc.
99 South Bedford Street, #7
Burlington, MA 01803-5169

Prepared for:

AEDC/DOTR
Arnold AFB, TN 37389

under Contract No. F40600-91-C-0010

Approved for public release; distribution is unlimited.

November 1991

TABLE OF CONTENTS

TABLE OF CONTENTS (Cont'd)

LIST OF ILLUSTRATIONS

LIST OF TABLES

U.S. DEPARTMENT OF DEFENSE

SMALL BUSINESS INNOVATION RESEARCH (SBIR) PROGRAM
PROJECT SUMMARY

TOPIC NUMBER: AF91-022

PROPOSAL TITLE: Raman Hydrogen Sensor (RHS) for Process Air Ducting

FIRM NAME: Spectral Sciences, Inc.

PHASE I or II PROPOSAL: I

Technical Abstract (Limit your abstract to 200 words with no classified or proprietary information/data.)

A fast-response (0.25 sec or faster) gaseous hydrogen (H_2) sensor is required in process air ducting at AEDC to support the testing of engines for the National Aerospace Plane. A sensitivity of around 0.1% H_2 over a sample pressure range of 2 to 15 PSIA is desired at humidity levels of up to 20% by weight.

In the Phase I Raman Hydrogen Sensor Program, Spectral Sciences, Inc. (SSI) has built and tested a breadboard laser Raman scattering instrument for H_2 concentration monitoring, and has demonstrated the feasibility of building a practical instrument that will meet the requirements of AEDC. All of the technical objectives were successfully accomplished. A detection limit of 0.0013 atm of H_2 using 18 mW of optical power was demonstrated, and the fundamental response time was found to be 0.3 sec at 1 atm with the current, non-optimized flow system. In addition, the feasibility of active subtraction of background water signals was demonstrated, and a conceptual design for a Phase II brassboard instrument was also developed.

Anticipated Benefits/Potential Commercial Applications of the Research or Development

The proposed Raman hydrogen sensor would improve safety in operations where liquid or gaseous hydrogen is used and presents an explosion hazard. In addition to AEDC, NASA applications may benefit from the improved time response of the sensor. The sensor may be highly valuable for the chemical industry, where large quantities of hydrogen are used for chemical processing.

List a maximum of 8 Key Words that describe the Project.

Raman	hydrogen
sensor	air
detector	laser
duct	NASP

Nothing on this page is classified or proprietary information/data

1. INTRODUCTION

1.1 Background

A fast-response gaseous hydrogen (H_2) sensor is required for operation in process air ducting at AEDC, to support the testing of engines for the National Aerospace Plane or other hydrogen-fueled vehicles. The system response should be no greater than 0.25 sec, and the sensor should be capable of measuring H_2 concentrations of 1% or greater by volume with a or better signal-to-noise ratio of 10:1 over a total pressure range of 2 to 15 PSIA.

The process air to be sampled originates from AEDC's ASTF engine test facility, where it may have a temperature of up to 1700° K and contain a large concentration of water vapor. As currently envisioned, the air sample will be passed through a water separator to cool it to around 100° C and remove excess water, making the sample compatible with a wider range of possible sensor materials. The water vapor content will still be considerable, up to 20% by weight (29% by volume in air). Thus the sensor must be insensitive to water vapor in order to prevent potential interference with the H_2 measurement.

Currently available sensors for real-time H_2 measurement include mass spectrographs, which are complex and costly, and catalytic combustion instruments, which may be sensitive to the flow rate, temperature and background gas composition and have a time response of seconds. These sensors are not suitable for AEDC's ASTF monitoring application. Spectral Sciences (SSI) proposes to develop a Raman Hydrogen Sensor (RHS) that uses laser scattering detection to achieve the required rapid response time and independence of the sample conditions, and which will be an accurate, sensitive, and low-maintenance instrument.

The proposed RHS instrument will build upon SSI's patented[1] Raman-scattering technology for H_2 detection, which has been used in prototype leak detection instruments built for NASA/KSC.[2] These instruments, designed for installation in the Mobile Launch Platform, have high sensitivity (better than 100 ppm), high vibration tolerance, and stable calibration (within several percent), and are equipped with remote control, diagnostic and other capabilities.

In the RHS Phase I program the RHS instrument concept has been successfully demonstrated in the laboratory, and a conceptual design has been developed for a brassboard to be built in Phase II. All of the Phase I technical objectives were met or exceeded. These included design and assembly of a laboratory breadboard apparatus, characterization of its response under variable sample conditions, characterization of its response to a H_2 transient, and development of the Phase II prototype design. Based on the Phase I results, we are confident that a practical Raman hydrogen sensor can be built for the fast-response, accurate and sensitive measurement of H_2 over the range of sample temperatures, pressures and humidities required for AEDC's application.

1.2 Basic Features of the Instrument

The RHS sensor measures hydrogen by detection of its characteristic Raman scattering when illuminated by a laser. A simplified schematic of the sensor is shown in Fig. 1. The laser light enters a chamber though which the gas sample is flowed; multipass optics are used to generate many traversals of the laser beam through the measurement region, increasing the light intensity. The H_2 in the sample generates Raman-scattered light that has a characteristic wavelength shift. This light is collected through a narrow-bandpass filter which rejects the non-shifted laser light as well as other undesired radiation, and it is detected by a photomultiplier tube. A chopper is used to modulate the laser light, permitting the use of lock-in electronics to acquire the Raman signal and reject ambient light and photomultiplier noise. The output of the lock-in circuitry is proportional to the H_2 density in the sample. By combining the lock-in signal with simultaneous pressure and temperature readings, the signal is converted to an instrument output in units of concentration (i.e., volume fraction).

The Raman technique has a number of advantages over many alternative approaches. The Raman scattering intensity is exactly proportional to the H_2 number density in the sample region, and is independent of the nature of the background gas. These properties allow complete calibration of the instrument using only two known gas samples. The time response is fundamentally limited only by the flow rate of the sample into the

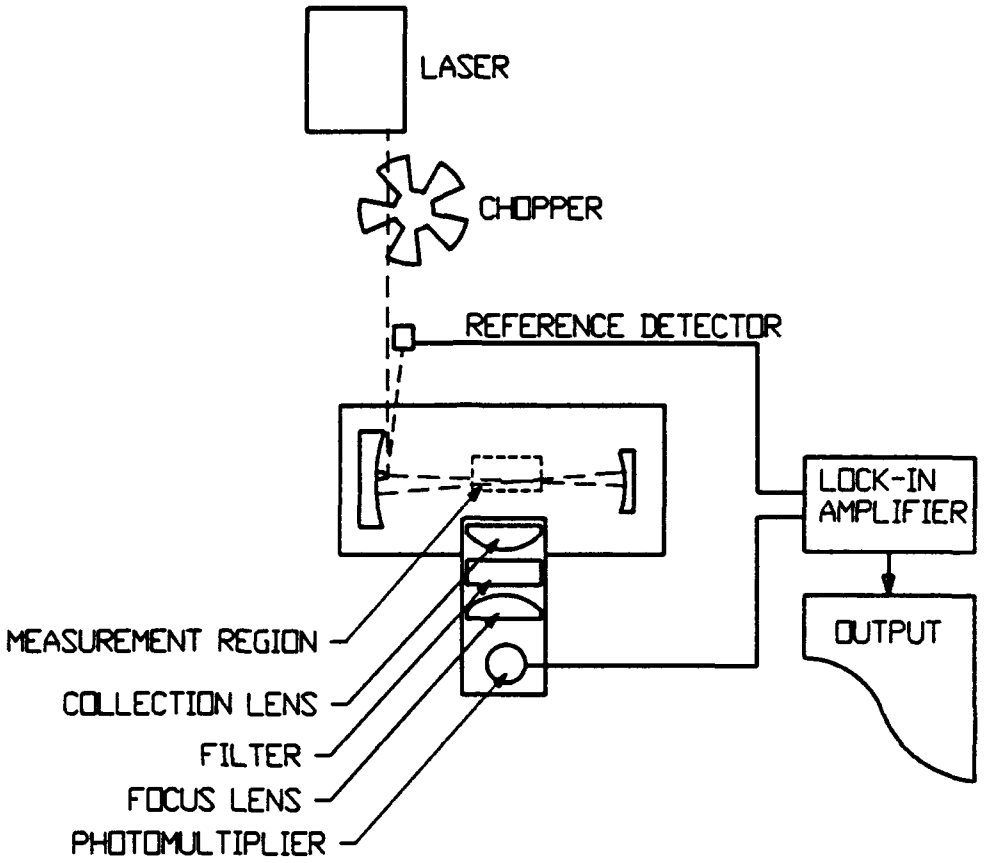

Figure 1. Simplified Schematic of RHS Sensor.

measurement region. All components comprising the RHS instrument are readily available. Recent advances in the size, cost, and reliability of both argon-ion and doubled-YAG lasers make the RHS approach highly practical.

1.3 Phase I Objectives

The overall objective of the Phase I effort was to provide a proof-of-principle demonstration of the proposed H_2 concentration sensor. This effort involved the assembly and testing of a laboratory breadboard system consisting of a laser, measurement chamber, gas-handling manifold, detection system, and associated electronics. The specific technical objectives were:

1. Design and assembly of a laboratory breadboard apparatus consisting of a Raman hydrogen sensor integrated with a high-flow, variable temperature and pressure gas sample delivery system;

2. Characterization of the response of the sensor under a representative range of pressures, temperatures and concentrations;

3. Characterization of the time response when the H_2 concentration is rapidly changed;

4. Conceptual design of a Phase II prototype RHS based on the Phase I findings and the anticipated operating conditions;

5. Preparation of a Final Technical Report.

The breadboard testing demonstrated the ability to measure H_2 concentration in air and other background gases over the required pressure range and with the required time response, as well as the ability to handle hot gas samples and to compensate for water vapor background signals. These tests also established the signal, background and noise levels, instrument sensitivity, and other parameters necessary for the development of a conceptual Phase II design.

1.4 Phase I Results

The detailed Phase I results are summarized in Subsection 2.3 and Section 4. In brief, the performance of the Phase I breadboard system was in good agreement with expectations. This makes us confident that the operation of the RHS is well-understood, and that the performance of a prototype RHS instrument can be accurately predicted from its design parameters. Specific accomplishments in Phase I include demonstration of a H_2 detection limit of 0.00013 atm using 18 mW of laser power (this corresponds to a S/N of 10:1 or better with 1% H_2 over the 2-15 PSIA total pressure range); demonstration of a fundamental instrument response time of 0.3 sec; demonstration of operation with very hot air samples (up to 180° C inlet gas temperature); demonstration of pressure-independence of the signal

down to 1 PSIA; and demonstration of the feasibility of cancelling background water vapor signals using active subtraction.

1.5 Organization of Report

This report describes the complete Phase I effort and results. Detailed descriptions of the laboratory breadboard design and testing are found in Section 2. The conceptual Phase II design is presented in Section 3. An overall summary of the Phase I effort, results and main conclusions is provided in Section 4.

2. LABORATORY BREADBOARD CONSTRUCTION AND PERFORMANCE TESTS

2.1 Description of Apparatus

The Phase I RHS breadboard apparatus was constructed by combining and modifying in-house mechanical and optical components, and interfacing them to a specially designed gas handling system, signal processing electronics and a computer data acquisition system. A schematic diagram of the Phase I apparatus is shown in Fig. 2. Details of the gas handling system, the sensor optics, the sample introduction method, and the data processing electronics are given separately below.

2.1.1 Gas Handling System

Flowing gas samples are obtained from compressed gas cylinders or a compressed gas mixed with room air. The sample gas flows down a 3/8" ID copper pipe that can be varied in length from 0.5 m to 15 m. The pipe can be heated as desired with a Bunsen burner or heat gun. Throttle valves in

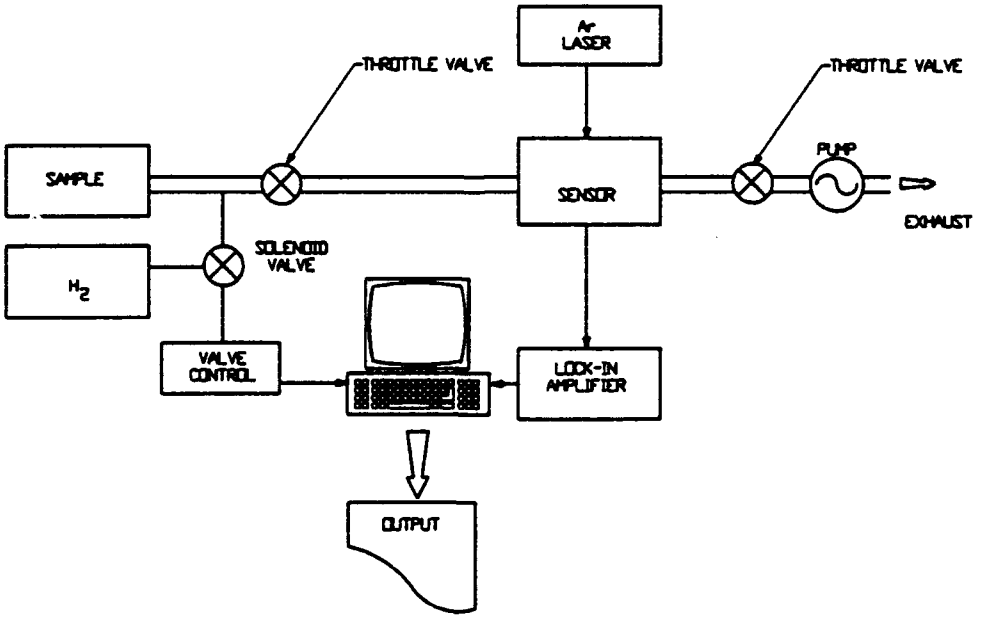

Figure 2. Schematic Diagram of RHS Phase I Apparatus.

the inlet and outlet pipes are used to vary the flow rate into and out of the sensor, and thereby control the pressure in the sensor. For some of the tests, a fine particle filter (Millipore WGFG06WB1, rated to 0.003 μm) and a coarse particle filter (Cambridge Valve and Fitting, rated to 60 μm) were placed in the inlet line directly upstream of the sensor. The sample gas exits the sensor via a 3/8" ID pipe that is normally connected to a 85 l/min (3 ft^3/min) mechanical pump (Gast DAA-P103-GB). By throttling the inlet flow, sub-atmospheric pressures as low as 2 PSIA were produced in the sensor and inlet line. As an option, the pump could be moved to the upstream side and used as a compressor to provide an atmospheric- or above-atmospheric pressure sample.

A 5.00% H_2/N_2 compressed gas mixture (Linde Primary Standard) was used to calibrate the instrument. Room air, pure helium, and pure nitrogen were used as background gases. For the time response tests, pure hydrogen was admitted via a sidearm located at the upstream end of the inlet pipe, where it mixed with a much larger continuous flow of room air or other background gas. A solenoid valve (Circle Seal Controls Model 649T-2PP-AA) was used to rapidly switch the hydrogen flow. The line current that powered the valve was also used to power a DC power supply, whose voltage was recorded on a personal computer along with the RHS instrument output. Switching the line current switched the valve and the DC supply on and off at the same time, so that the DC voltage served as an accurate timing indicator for the valve position. Since the room air flow was much greater than the pure hydrogen flow through the sidearm, the system pressure was not appreciably perturbed by the hydrogen flow.

2.1.2 Sensor Optical System

A detailed diagram of the breadboard optical system is shown in Figs. 3a and 3b. The principal components are an air-cooled argon ion laser, a measurement chamber containing a multipass optical cavity, and an imaging system with a bandpass-filtered photomultiplier tube (PMT) to collect the Raman-scattered light. The argon ion laser (Omnichrome Model 532) has an output of 8 to 20 mW at 488 nm, depending on the current level; it was typically operated at 8 mW or 18 mW. The optical components are

supported on a 1/2" thick aluminum base plate and a perpendicular 1/2" thick aluminum bulkhead. The bulkhead supports the chamber, collection and detection optics, and optical rails for the multipass cavity mirrors.

As shown in a horizontal cross-sectional view in Fig. 3a, the beam from the laser (1) is directed via a pair of dielectric-coated flat mirrors (2) on adjustable mounts through a chopper wheel (3) and through a 150 mm F.L. lens (4) mounted on the vertical bulkhead (5) into the measurement chamber (6). There the beam is directed into a multipass optical cavity via a 3 mm wide front-surface reflective prism (7) mounted next to the front cavity mirror. The multipass cavity is defined by a pair of dielectric-coated concave mirrors (8,9) having radii of curvature of 100 mm (front) and 75 mm (rear) and diameters of 50 mm (front) and 25 mm (rear). The mirror dimensions and spacing were chosen to adequately separate adjacent beams near the prism and sufficiently isolate the collection optics from stray light, while minimizing the chamber volume. The rear mirror is on an adjustable mount, and both mirror mounts are affixed to 3/8" diameter stainless steel rails (10).

With the cavity mirrors separated by a distance just under the sum of their radii of curvature, the cavity is of the type described by Herriott[3] and later used by several other workers in Raman applications (e.g., Trutna and Byer[4]). In this configuration the laser beam repeatedly traverses the cavity, forming an ellipse of spots on each mirror and an intensely illuminated focal region in the center of the cavity where each pass of the beam comes nearest to the optical axis. The distance between the mirrors is set according to the "reentrant condition"[3] in which the beam returns to its original location on the prism after a chosen number of passes (here set to 30). The beam then exits the measurement chamber and falls on a photodiode (11) whose output provides an indicator of correct optical alignment, as well as a phase-locking reference for the signal-processing electronics. To isolate the Raman light collection optics from stray laser light scattered by the cavity mirrors and prism, a pair of adjustable baffles (12) is placed between the mirrors and the cavity focal region, and the mounts, baffles and chamber walls are anodized black.

The collection optics system is shown in vertical cross section in Fig. 3b. The Raman-scattered light from the focal region is imaged onto the photocathode of a multialkali PMT (Hamamatsu H957-08) (17); the long

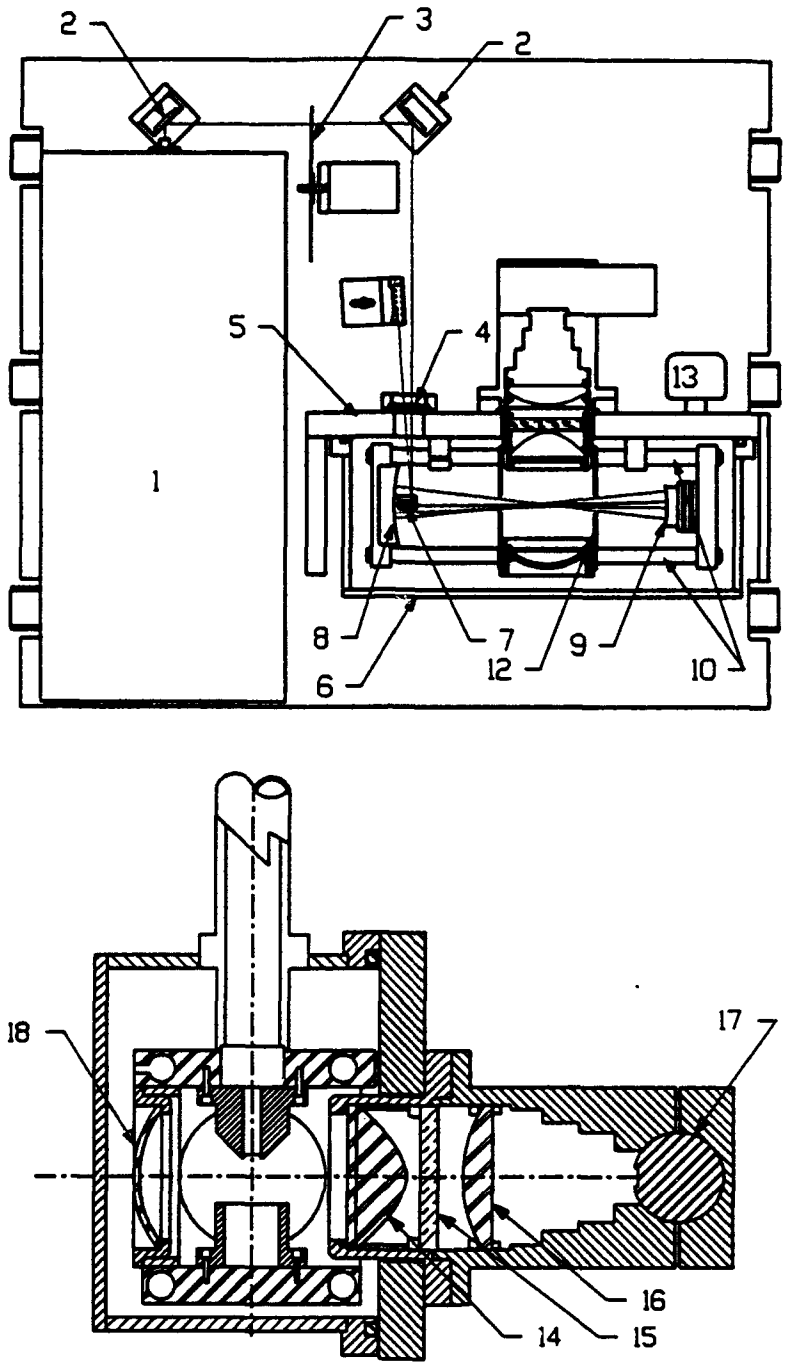

Figure 3. (a) Top Cross-Sectional View of Breadboard Sensor. (b) Side Cross-Sectional View of the Measurement Chamber and the Imaging Optics.

dimension of the photocathode is parallel to the optical axis of the cavity. The magnification ratio and numerical aperture of the optics were chosen to optimize the light collection efficiency. The lenses consist of an anti-reflection-coated 50 mm diameter 41 mm F.L. aspheric plano-convex collection lens (14) which collimates the Raman light through a bandpass interference filter (15), and a 50 mm diameter 63 mm F.L. spherical plano-convex lens (16) which refocuses the light onto the PMT photocathode. Discrimination of the H_2 Raman signal from stray laser light, Raman scattering from the carrier gases, and background fluorescence is accomplished by a bandpass interference filter (60% transmission, FWHM = 10 nm in the current brassboard) centered on the Q branch of the Raman band of H_2 at 612 nm. The filter consists of a 3-cavity dielectric filter sandwiched with a colored glass blocking filter, and is oriented with the dielectric side towards the sample. Light collection is further enhanced by a 50 mm diameter, 19 mm F.L. concave front-surface mirror (18) mounted on the opposite side of the focal region to direct the rear-scattered Raman light back through the focal region and towards the lens system.

2.1.3 Sample Introduction

In the design used in previous work,[2,5] the sample gas was introduced into the focal region via a flow injector located above the optical axis, after first flowing through a feed tube that led from a gas inlet located on the vertical bulkhead. A sintered tube array straightened the sample flow to provide a laminar flow stream at the injector exit, and flow deflector placed opposite the injector redirected the flow back towards the focal region. For the current investigation, we modified the breadboard to eliminate the sintered tube array and feed tube, allowing a shorter and straighter flow path into the focal region. A hole was machined in the top of the chamber; a 3/8" ID (1/2" OD) inlet tube was inserted through the hole via Swagelok fittings, extending down towards the focal region. We presumed that this arrangement would permit a more rapid introduction of the sample through the measurement region, improving the time response of the instrument.

Several variations of this basic sample flow arrangement were tried. These included letting the sample exit from the bottom of the chamber

through an outlet tube directly opposite the inlet tube, letting the sample exit through the bulkhead, and confining the flow through the focal region using a pair of glass microscope slides. The glass slides were placed vertically on either side of the flow stream and were kept far enough away from the laser beams to prevent direct scattering of the beams. The Raman-scattered light was transmitted through the slides to the collection optics.

Initial tests revealed that the initial response to a hydrogen transient was similar with all of these flow arrangements. However, the final reading was reached more rapidly by letting the sample exit through the bulkhead, as in our original design, rather than through the bottom of the chamber. These observations are discussed and explained in Section 2.2.3. The addition of the glass slides made essentially no difference in the time response. Since the slides somewhat increased the background signal from scattered light, they were not used in further work.

2.1.4 Electronics

Processing of the PMT signal is accomplished with analog circuitry based on a commercial lock-in amplifier board (Evans Electronics Model 4110). Modifications of the original signal processing circuitry(2) were made to reduce the integration time constant from 1 second to 0.1 second. Inputs from temperature and pressure sensors (the latter is item (13) in Fig. 3a) are used to normalize the signal to yield an analog output voltage that is proportional to fractional hydrogen concentration. Normalization of the signal to the laser intensity is not required since the laser is actively controlled to eliminate fluctuations and drift.

Permanent records of the signal are made using either a chart recorder or a personal computer. In the latter case, the signal was sent to an analog-to-digital converter of a lock-in amplifier (Princeton Applied Research 5209), and the lock-in's software was used to record the signal versus time along with other desired instrument outputs such as pressure or the valve timing voltage.

2.2 Performance Characterization

2.2.1 Signal and Noise Levels

An important part of the Phase I work was to characterize the signal and noise levels as a function of H_2 concentration and other sample characteristics and conditions. This work is described in detail below.

2.2.1.1 General Characteristics

As found in our earlier work on Raman hydrogen sensors,[2,5] the output from the RHS sensor was found to contain three basic components:

1. Small, constant background signal and noise levels in the absence of H_2. The background signal results from scattered light, and is nulled out by properly zeroing the instrument. The background noise arises primarily from photomultiplier dark current noise, with an additional component due to electrical pickup.

2. A hydrogen signal component that is proportional to the H_2 concentration. This is the Raman scattering signal.

3. A noise component that increases slowly with increasing H_2 concentrations. This is the "shot noise" component associated with the photon collection statistics, and scales with the square root of the optical signal.

In addition, occasional spikes in the signal were found when sampling unfiltered room air, and are ascribed to dust particles. The inlet line filters removed these spikes, but did not significantly affect the overall noise level or other aspects of the RHS breadboard performance.

Representative traces of the signal versus time for a 1 atm (14.7 PSIA) sample are shown in Fig. 4. These measurements were made with different inlet pipe lengths and with the lowest laser power of 8 mW, for which the noise levels are the largest and most visible. Room air was flowed through the main manifold; pure H_2 gas was introduced via the sidearm by opening the solenoid valve at time t=0. The typical ratio of air to H_2 flows was 20:1, which gave a H_2 concentration close to that of the reference 5%

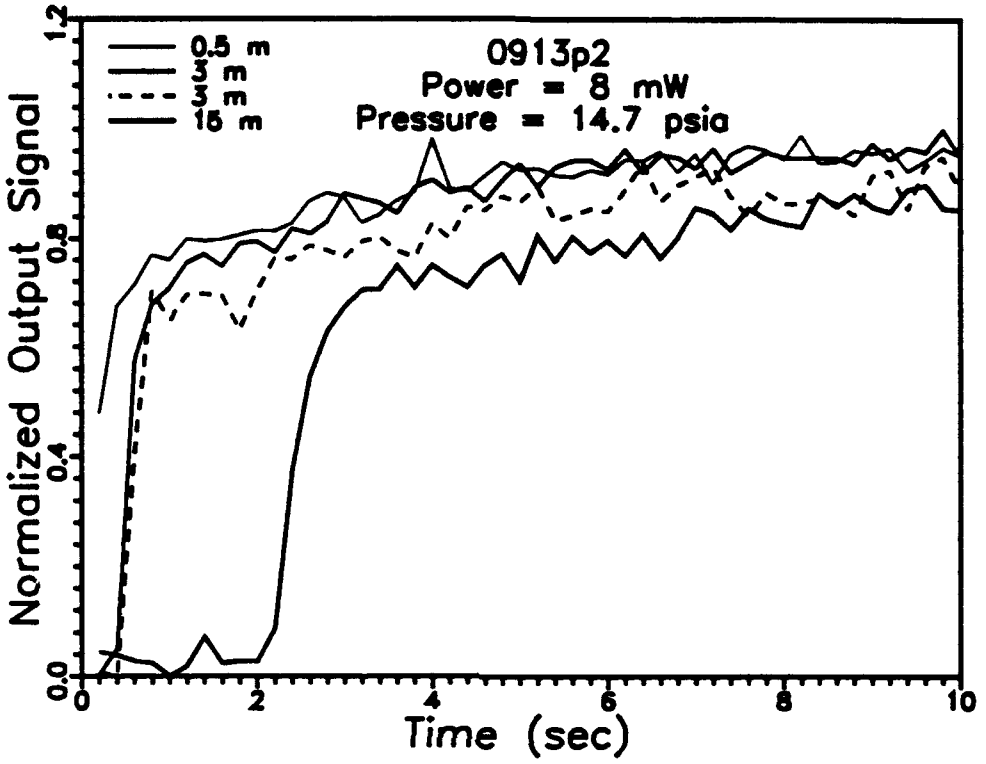

Figure 4. RHS Signal Versus Time After Introduction of 5% H_2/N_2 Mixture, Using Different Inlet Pipe Lengths. Total Pressure = 1 atm (14.7 PSIA), Laser Power = 8 mW.

mixture. These traces have been analyzed to determine the time response as a function of pipe length (see Subsection 2.2.3), as well as the signal-to-noise ratio. With this ~5% H_2 concentration, the signal-to-noise ratio is around 25:1.

Other examples of data are shown in Fig. 5. Here, a higher laser power of 18 mW was used and a better signal-to-noise level is obtained at a similar pressure and H_2 concentration. In accord with paragraph three above, a slightly smaller noise level is found with zero or very low hydrogen concentrations due to the absence of shot noise.

2.2.1.2 Observed and Calculated Sensitivities

The results of a computer analysis of traces such as those in Figs. 4 and 5 are summarized in Table 1. The RMS noise level is given in terms of

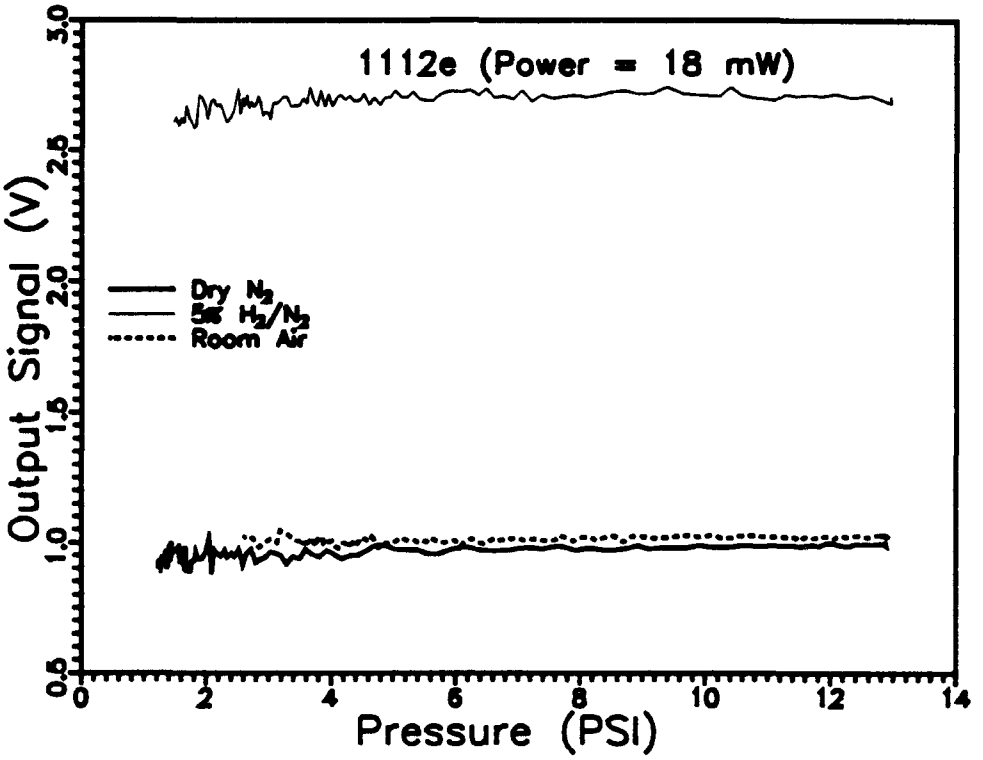

Figure 5. RHS Signal as a Function of Total Pressure for Room Air, Pure Nitrogen, and 5% H_2/N_2 Samples; Laser Power = 18 mW.

Table 1. Observed and Predicted RMS Noise Levels

H_2 Concentration	Laser Power	RMS Noise (% H_2 at 1 atm) Predicted	Observed
0%	8 mW	0.025	0.05
	18 mW	0.011	0.013
5%	8 mW	0.055	0.08
	18 mW	0.037	0.05

the equivalent H_2 density in percent at 1 atm, which may be taken as the effective instrument sensitivity. Also shown in the Table are predictions based on previous observations and calculations[5] for the same optical system with a 1 second electronics time constant τ, where a detection limit of around 80

ppm (0.008 % atm) H_2 was estimated for a laser power of 8 mW. The predictions for the current RHS instrument have been made by scaling from those calculations, accounting for the actual laser power (8-18 mW) and τ (0.1 sec) in the current system. The Raman signal is proportional to the laser power, while the noise scales with $1/\sqrt{\tau}$.

According to the Table 1 predictions, increasing the laser power from 8 to 18 mW should improve the instrument sensitivity by around a factor of 2, to around 0.011%, in the low-H_2 limit, but by a slightly smaller factor at 5% H_2, where the shot noise contribution scales inversely with the square root of the laser power rather than with the power. The measured noise levels are not precisely reproducible, making it difficult to distinguish these slightly different behaviors. Still, the overall agreement between the measurements and the predictions is reasonably good, the average noise level exceeding the predictions by around 50%.

2.2.1.3 Pressure-Dependence of Sensitivity

Since the Raman signal is proportional to hydrogen density, the instrument sensitivity expressed in terms of atm H_2 is identical at all pressures. However, since at low pressures the density is reduced, the sensitivity expressed in fractional concentration units is proportionally reduced. The RHS electronics effectively convert the signal to concentration units; this leads to a noisier output at lower pressures, as illustrated in Fig. 5.

In conclusion, the sample pressure needs to be considered in determining the minimum required laser power for a given application. For example, the 0.013% H_2 sensitivity at 1 atm (14.7 PSIA) and 18 mW of laser power translates to a sensitivity of 0.08% at 2 PSIA. This is still sufficient for AEDC's monitoring application.

2.2.2 Total Pressure Variation Effects

The RHS response was tested over the 1-15 PSIA range using the 5% H_2 mixture and hydrogen-free background gases. Typical results are shown in Fig. 5, which were obtained using samples of room air, N_2, and 5% H_2, and a laser power of 18 mW. In this experiment the sample pressure was slowly

reduced from 13 PSIA down to 1 PSIA by throttling back the sample flow while the instrument was pumped down; the pressure gauge reading was recorded simultaneously and is displayed on the x axis. The signals from all three samples show virtually no variation over the entire pressure range. It should be noted that the raw optical signal, which is proportional to the H_2 density, is made proportional to concentration units by dividing by the output from the pressure gauge. The observed pressure-independent behavior of the RHS output confirms the proper operation of the signal processing circuitry, and also confirms that optical alignment is maintained despite the large forces exerted on the measurement chamber while under partial vacuum.

2.2.3 Time Response

The time response of the RHS breadboard was determined from measurements such as those shown in Fig. 4. The Fig. 4 measurements were made with a 1 atm (14.7 PSIA) total pressure, with the sample gas entering the chamber through a variety of inlet tube lengths L ranging from 0.5 m to 15 m, and exiting through the bulkhead. The 67% time response (time to 67% of full deflection) determined from these traces fits the formula $0.3+0.18L$ seconds. Similar measurements were made at 2 PSIA by throttling back the air and H_2 flows. The response is about 2 times slower, indicating a reduced flow speed at this lower system pressure.

Other measurements were made to test the effect of different flow configurations. Virtually identical results were obtained with and without the gas filters on the inlet line. This is not surprising, since with the 3/8" ID inlet line used in Phase I, the internal volume of the filters is small compared with that of the line. A comparison of the time response with the sample exiting through the bottom outlet or through the bulkhead (side outlet) was also made early in the test program before the solenoid valve had arrived. These results are shown in Fig. 6. Since timing signals were unavailable from the manual valve used, the x-axis was aligned to start the H_2 signal transients at $t = 0$.

As seen in Fig. 6, the initial rise to 67% of the full signal of 1.0 is reached within less than 0.3 sec with both flow configurations. The major difference is that with the bottom outlet configuration, the full deflection is

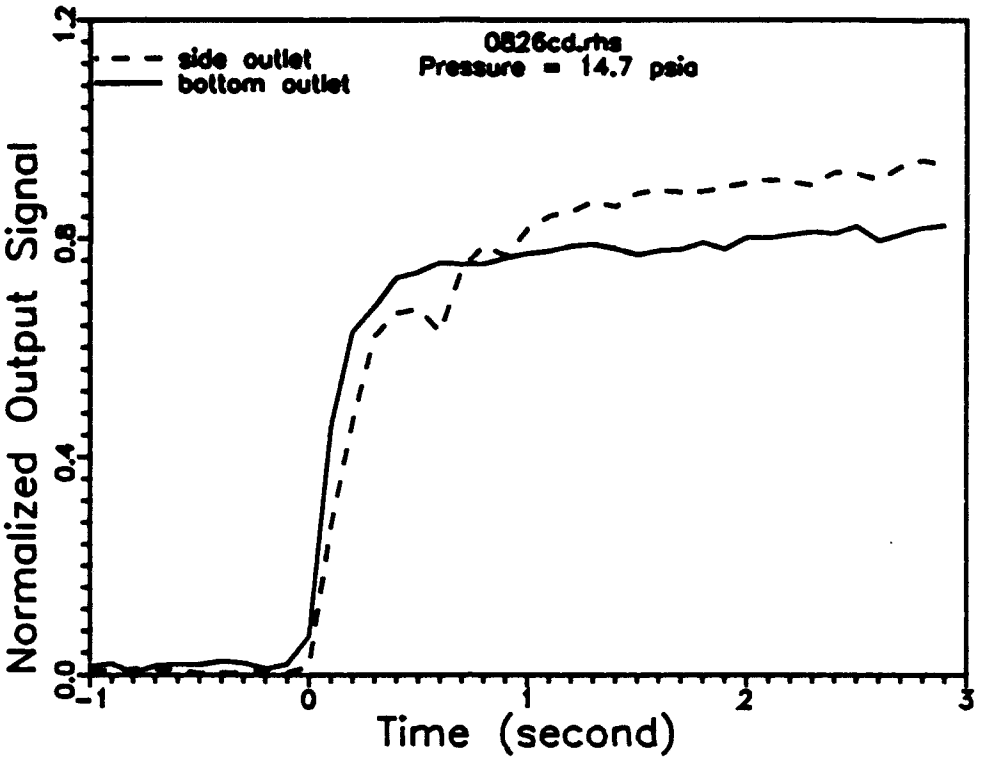

Figure 6. RHS Signal Response to a H_2 Transient Using Different Outlet Configurations. Full Signal is Normalized to 1.0.

not reached for many seconds, whereas with the side (bulkhead) outlet configuration, it is reached within 2-3 seconds.

Our interpretation of these results is that the rapid initial rise is associated with the establishment of a laminar jet of sample gas from the inlet pipe, while the slower rise thereafter is due to the optical signal from surrounding areas that are flushed by turbulent mixing. By blocking off the bottom outlet, the sample gas is deflected back towards the focal region and thus promotes more rapid mixing outside the jet. The reason for the large contribution to the signal from outside the jet is the small diameter of the inlet pipe (3/8" ID) compared to the length of the focal region imaged onto the PMT (2 cm, or around 3/4"). In Phase II, the inlet pipe will be flared to a 3/4" ID; this should permit a rapid response time with either flow configuration.

To summarize the results, we found a fundamental RHS time response of 0.3 seconds using a 3/8" ID inlet tube and an 85 l/min (3 ft^3/min) mechanical pump in Phase I. This essentially satisfies the proposed AEDC application requirement. Not surprisingly, the total time response is limited by the transit time down the inlet tube, which indicates that careful consideration needs to be given to the flow characteristics of the inlet line and water separator to which the RHS instrument would be attached.

According to AEDC personnel, much more rapid flow rates (around 100 ft/sec or 30 m/sec) are readily obtained by using a much smaller (e.g., 1/4" OD) inlet pipe. The drawback is that a larger pressure drop between the duct and the RHS instrument is required, reducing the pressure in the measurement chamber to as low as 1 PSIA and thus reducing the instrument sensitivity. However, this loss in sensitivity can be compensated by an increase in laser power in Phase II.

2.2.4 Water Vapor Response

In the proposed monitoring application at AEDC, the process air samples are expected to contain a large amount of water vapor. We can estimate the effect of water vapor on the RHS signal based on measurements comparing room air with a dry background gas. For example, in Fig. 5 the room humidity signal is equivalent to around 0.14% H_2. Since the water vapor concentration in the room was about 1.5%, the ratio of responses to equal concentrations of water vapor and hydrogen is 11:1 in the RHS breadboard. In the proposed AEDC application, the water vapor background signals would likely be over an order of magnitude larger, and therefore similar in magnitude to the expected hydrogen signals.

The water background signal arises from the tail of the ν_1 Raman band that overlaps the wavelength region transmitted by the H_2 bandpass filter. The magnitude of this signal therefore depends on the width of the filter bandpass. In previous work where we used a narrower (5 nm FWHM) filter,[2,5] we obtained a 50:1 H_2/water response ratio, nearly five times better than in the current RHS breadboard. Better discrimination would be possible using a still narrower bandpass. Still, there is a practical limit to the

narrowness of the bandpass that can be used without significantly reducing the hydrogen Raman signal.

An effective method of compensating for the water background signal would be to subtract an equivalent signal determined from the simultaneous measurement of Raman scattering at the ν_1 peak wavelength using a second set of collection optics. We investigated the feasibility of this approach in Phase I, as described in the following subsection.

2.2.5 Water Vapor Compensation

To demonstrate the feasibility of the proposed water background subtraction approach, we performed measurements with room air, dry nitrogen, and 5% H_2 using a 594 nm (4.4 nm FWHM) bandpass filter, which transmits the water ν_1 Raman scattering, in place of the H_2 Raman filter. Both filters have essentially the same peak transmission of ~60%. From the average room humidity of 1.5% by volume, and the measured 594 nm signal level of 0.185 V, equivalent to 0.925% H_2, we derive a water/H_2 detection efficiency ratio of 0.62. This value is in good agreement with the relative Raman cross sections for these two molecules reported in the literature.(6)

The 5% H_2 mixture was found to give a small signal of 0.078 V at 594 nm. Comparing this value with the water signal, this represents an 8:1 discrimination ratio for water versus hydrogen at 594 nm.

From the above measurements, and assuming a 50:1 H_2/water response ratio with a 5 nm H_2 bandpass filter, we may write the net signals in volts in the water (594 nm) and H_2 bandpasses, respectively, as

$$S_w = 0.123C_w + 0.0156C_h \quad (1)$$

$$S_h = 0.200C_h + 0.0040C_w \quad (2)$$

where C_w and C_h are the respective concentrations in per cent of water and hydrogen, and the H_2 response calibration is defined as 0.2 V per 1% H_2. Solving these equations yields the hydrogen concentration as a linear combination of the two bandpass signals,

$$C_h = 5.01(S_h - 0.0325S_w) \quad (3)$$

According to the above result, the water background signal in the H_2 bandpass is exactly cancelled by subtracting the 594 nm signal times a scale factor of 0.0325.

The very small value of the background subtraction scale factor insures that any noise or calibration uncertainty in the 594 nm channel would not introduce any significant uncertainty in the hydrogen concentration measurement. For example, if there were as much as 50% water vapor in the sample, the water background would be the same size as a 1% H_2 signal. Since the noise level will be less than 1% of this, and the subtraction accuracy should also be around 1% or better, the total background subtraction error should be on the order of a few hundredths of a percent of H_2. This is well within the desired instrument accuracy. We conclude that the proposed water background subtraction approach would be highly effective.

2.2.6 Response to Temperature Variation

Several tests of the breadboard RHS system were made with heated room air samples. For safety reasons, we were reluctant to apply heat while using either pure hydrogen or the 5% mixture. Hot flows of room air could be introduced into the system in two ways, either by heating the inlet pipe with a Bunsen burner, or by directly sampling the exhaust from a heat gun. Most of the work was performed using the latter method, which was more convenient and allowed higher gas temperatures to be reached. While these tests did not permit us to check the calibration of the sensor, they did provide information on the instrument zero reading, which is sensitive to the optical alignment. As long as the correct optical alignment is maintained, we expect that the hydrogen response calibration is maintained as well.

In tests using the heat gun as the hot air source, the instrument output and the reading of the temperature sensor were recorded versus time. The temperature sensor is a thermocouple fed through the vertical bulkhead into the measurement chamber. Due to conduction through the thermocouple mount, it probably measured a weighted average of the gas temperature in the chamber and the bulkhead temperature. The actual temperature of the heat

gun exhaust is about 180° C in open air, and could have been even higher in our test due to constriction of the air flow by the inlet tube. Since this temperature is much greater than the sample temperatures expected in the AEDC application (estimated to be 100° C or less), this test was considered quite severe.

The test results are shown in Fig. 7a. The heat gun was turned on for 8 minutes, during which time the instrument temperature rose to 60° C. The heat gun was shut off for four minutes and was then turned on again. During both heating periods the RHS signal rose smoothly from its zero reading, with little change occurring during the first few minutes when the temperature reading was below 40° C. The RHS signal recovered very quickly when the heat was shut off. Between the heat gun shutoff and the second rise, the RHS maintained its original zero reading while the thermocouple indicated between 40° and 55° C.

The behavior of the RHS signal below the 50° C reading is shown more clearly in Fig. 7b, where the data are replotted as equivalent H_2 concentration versus measured temperature. It is seen that below 40° C, the signal shows very little drift, and after the heat gun shutoff, the signal at up to 50° C was unchanged from its room temperature reading.

Our interpretation of these measurements is that the optical alignment of the RHS is not directly sensitive to the sample gas temperature, which changed within seconds as the heat gun was turned on and off, but it is sensitive to differential thermal expansion due to non-uniform heating of solid surfaces of the instrument, such as when the heat gun had been turned on for several minutes. The thermal gradients dissipate rapidly via conduction when the heat source is removed, although the instrument remains warm. We therefore expect that as long as a reasonably uniform instrument temperature is maintained, such as by pre-heating the instrument, the optical alignment should be unaffected.

It should be emphasized that no effort was made in the Phase I design to minimize either temperature gradients or thermal expansion coefficients. In the Phase II design and the subsequent field instrument, the measurement chamber will be maintained at a uniform temperature close to that of the incoming sample, and components currently fabricated from aluminum will be constructed of stainless steel, which has a much smaller thermal expansion

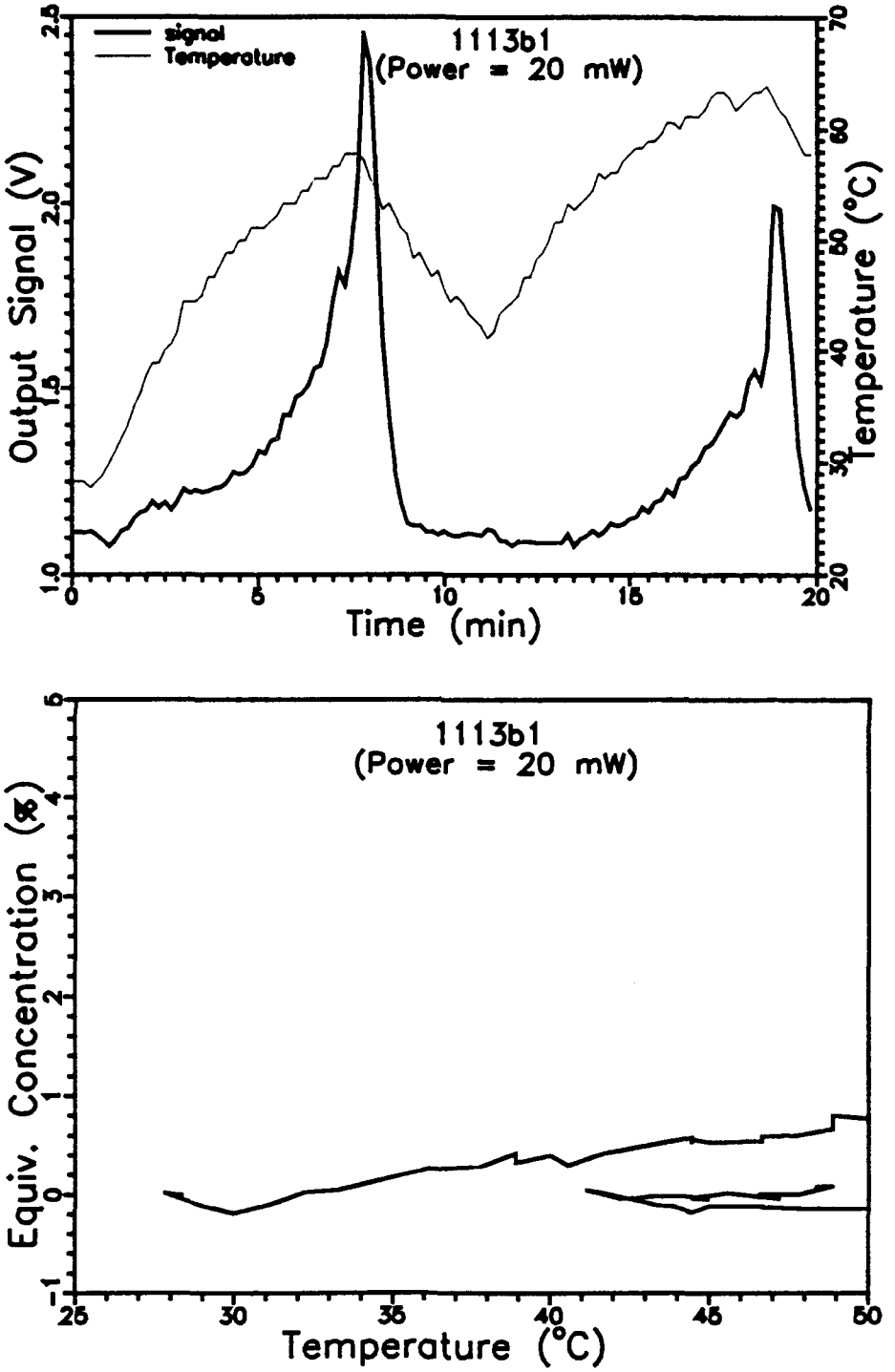

Figure 7. RHS Signal and Chamber Temperature Response to 180° C Air From a Heat Gun. (a) Readings Versus Time; (b) H_2 Equivalent Signal Versus Temperature.

coefficient. Stable operation should then occur for sample temperatures well above that observed in the Phase I tests.

2.3 Summary and Conclusions

The concept of using Raman scattering for rapid, sensitive and accurate detection of hydrogen concentrations in process air samples has been successfully demonstrated in the laboratory. A laboratory breadboard instrument and gas handling manifold were built and tested in the RHS Phase I program. The H_2 concentrations, gas temperatures, and total pressures were representative of anticipated air samples from AEDC's ASTF engine test facility. The feasibility of active subtraction of the anticipated background moisture signal using a second optical channel was also demonstrated. The key findings were as follows:

1. A sensitivity limit of 0.00013 atm H_2 (0.013% at 1 atm) was demonstrated with a laser power of 18 mW, attainable with our current air-cooled argon ion laser. This translates into a minimum signal-to-noise ratio of 10:1 for an H_2 concentration of 1% over the anticipated pressure range of 2 to 15 PSIA. Except at high H_2 concentrations (greater than a few percent), proportionally improved sensitivity is obtained with increased laser power. In addition, the instrument response was measured using H_2-containing and H_2-free gas samples over the pressure range of 1 to 15 PSIA, and found to be pressure-independent.

2. A fundamental instrument response time of 0.3 seconds was demonstrated with the current laboratory apparatus. The overall response time was limited by the flow time through the gas handling system. Using an inlet pipe several meters long, a system response time of under 1 second was demonstrated using a pumping rate of 85 l/min obtainable from a small mechanical pump. A higher pumping rate would result in a faster response.

3. The instrument was operated with a hot (180° C) air sample, much hotter than would be expected at AEDC where a water separator would be used in the sample line. No degradation of the instrument occurred, and proper operation was observed at instrument temperature readings of up to 55° C under thermal equilibrium conditions and up to 40° C under nonequilibrium conditions.

4. The background signal contribution due to water vapor in the sample has been characterized. Comparing the results with previous measurements using a narrower optical bandpass filter, the background signal level is found to have an inverse correlation with the width of the bandpass, as expected. A method for subtracting the water background signal using a second optical channel was investigated and shown to be feasible. With this approach, even very high levels of water vapor will not pose a problem for the RHS instrument.

The Phase I findings demonstrate that a successful RHS H_2 sensor can be built for AEDC's process air monitoring application. A few issues which were beyond the scope of the Phase I investigation need to be addressed in Phase II. While the full sampling pressure and temperature ranges were tested in Phase I, the apparatus was originally designed for room-temperature operation and needs to be modified to provide a heated measurement chamber that will permit continuous operation at 100° C. In addition, in Phase I the sample humidity was restricted to room air levels and below. Selecting the optimal Phase II design parameters may require the specification of more precise sampling conditions than our current estimates. The particulate content in the process air samples and the instrument's tolerance to it may be difficult to estimate, but they should be resolved by a field test in Phase II.

The proposed Phase II brassboard prototype instrument is described in the next section, and is very similar to the Phase I breadboard. This similarity, and SSI's past experience in constructing similar Raman instruments, means that the prototype can be constructed and field-tested in a timely manner in Phase II. These tests will provide us with an accurate assessment of the instrument capabilities and an opportunity for any needed design revisions early in the development process.

3. PHASE II DESIGN

In this section we present a conceptual design for a Phase II brassboard Raman Hydrogen Sensor. The optical design of the Phase II instrument closely follows the proven design of the Phase I breadboard system. The goal of the Phase II effort is to develop a prototype instrument for field testing at AEDC's ASTF engine test facility.

It is anticipated that the RHS instrument will be installed outside the duct on a sample line downstream of a water separator. It would therefore be designed for compatibility with humid, warm air samples, and would be adequately sheltered from the outdoor environment. As the water separator system has not been operationally tested, certain conditions such as the water content, particulate levels, and flow rate are not precisely established. Thus, some modifications of the following design may be ultimately required.

3.1 Design Considerations

The Phase II brassboard instrument will be similar in design to the Phase I breadboard, with the major thrusts of Phase II being an upgrading of the optical system for better sensitivity and for cancellation of the water vapor signal, the design of a heated measurement chamber, and the integration of the components into a rugged package. Additional features that can be built in as desired include means for remote operation, in-line calibration, and fault diagnosis. The specific design goals can be summarized as follows:

- Maintain H_2 sensitivity and provide humidity compensation
- Preserve rapid response time
- Accommodate the desired temperature and humidity range
- Provide on-line calibration means
- Minimize required maintenance
- Provide additional features as required (remote operation, fault diagnosis, etc.)

Some specific approaches for meeting these goals are described below.

3.1.1 Sensitivity

The sensitivity of the instrument is directly related to the laser power and wavelength, the sample pressure, the efficiency of the collection optics, and the integration time of the electronics. Using an air-cooled, 488 nm argon ion laser operated at 18 mW, and an integration time of 0.1 sec, the Phase I breadboard achieved a sensitivity of 0.013% H_2 at 1 atm pressure, corresponding to an 0.1% or better concentration sensitivity over the 2-15 PSIA pressure range. This sensitivity is similar to what would be desired in the prototype instrument. However, in Phase II some degradation of the sensitivity may arise from two sources. To increase the sample flow velocity in the inlet tube, it may be necessary to use a narrower (e.g., 1/4" OD) tube which would reduce the minimum pressure in the sensor from 2 PSIA to 1 PSIA, leading to a corresponding reduction in the density of H_2 to be measured. Secondly, since a second optical channel at 594 nm (for water vapor background subtraction) will be included in the Phase II instrument, geometrical constraints may result in up to a 50% reduction in the collection efficiency in each channel.

To compensate for such sensitivity losses, we propose using a more powerful, but otherwise similar, air-cooled argon ion laser. For example, a commercially available 150 mW laser (e.g., Omnichrome Model 543) would provide eight times the power used in Phase I, and thus factor-of-four or better signal-to-noise ratios compared to the same conditions in Phase I.

3.1.2 Time Response

The fundamental response time of 0.3 sec demonstrated in the breadboard instrument should be satisfactory for Phase II. A slightly faster response time is anticipated from widening the flow inlet above the focal region to match the 3/4" length of the region imaged onto the PMT.

The total time response of the installed system will be limited by the flow time through the sample line provided by AEDC. To best preserve the fundamental instrument response, the diameter of the sample line, the choice

of gas filter(s), and the design of the water separator should be carefully reviewed by both AEDC and SSI engineers. Further discussion of the flow configuration appears in Section 3.2.3.

3.1.3 Sample Compatibility

The expected sampling temperature is expected to range from ambient temperatures up to around 100° C. Water vapor content may be up to 20% by weight (29% by volume in air), and total pressures may range from 15 PSIA (1 atm) down to 2 PSIA (0.14 atm).

Compatibility with the anticipated range of sampling temperatures and humidities will be achieved by heating the measurement chamber. The chamber temperature will be slightly above 100° in order to prevent condensation. Uniform heating will also minimize thermal gradients that can cause optical misalignment. As with the Phase I system, the chamber will be air-tight to permit sub-atmospheric pressure operation.

The use of active background subtraction (see Subsection 2.2.5) will eliminate any background signal due to water vapor even at the highest anticipated humidity levels. This method should also be effective for eliminating background scatter caused by a small quantity of water aerosol (droplets), since the Raman spectra of gaseous and liquid water are similar. However, a significant quantity of droplets is not expected at 100° C. A more likely source of background scattering is from solid particulates. A large number of these should be removed in the water separator. A course filter, such as the one used in Phase I, will effectively remove remaining dust particles. A fine particle filter, such as the Millipore filter used in Phase I, was found to make little difference in the instrument performance and should not be required. The gas filter plumbing will be designed for easy filter replacement.

3.1.4 Calibration

Long-term stability of the calibration is required for continuous operation over many hours, and to minimize or eliminate calibration shifts in between operating periods. We have previously demonstrated the stability of a similar

Raman hydrogen sensor, designed for ambient temperatures, during continuous operation over one week and during intermittent operation over many months.(2) Furthermore, the Phase I temperature tests revealed no significant instrument drift at temperatures of up to 40° C, and suggest that with proper chamber design in Phase II, the instrument will be stable at higher temperatures than this.

The calibration procedure is very simple, since the instrument responds linearly. It consists of setting zero and span potentiometers in the amplification circuit to give the correct readings with a hydrogen-free and a hydrogen-containing compressed gas. Alternatively, if it is inconvenient to reset the potentiometers, the output signals from these calibration gases can be noted and utilized to correctly interpret the instrument readings, and therefore to properly set an alarm point for a desired H_2 concentration. The latter procedure can be performed rapidly and remotely, without the need to access the instrument (see Subsection 3.1.6), and thus could be performed if desired in the midst of data-taking.

3.1.5 Maintenance

A low-maintenance instrument is desired. The design goal is for routine maintenance to consist of drainage of water traps, periodic replacement of any inlet line filters, and occasional cleaning of the optics. The flow configuration will be designed to minimize fouling of the optics, particularly the cavity mirrors (see Section 3.2.1). The lifetime of the laser plasma tube varies with the operating current and hence the power output, but is expected to be between 5,000 and 10,000 hours of use, which is sufficient to insure many years of service.

3.1.6 Additional Features

Several features contained in SSI's earlier prototype Raman sensor built for NASA/KSC(2) could also be incorporated in the Phase II RHS prototype. These include dual output channels for high and low ranges, logical diagnostic outputs, and a remote interface for control, diagnosis and readouts. The remote control capability may include turning the laser on and off and

switching between sample or calibration gases. One or more logical diagnostic outputs would provide true/false readings to indicate proper instrument operation. A threshold indicator on the intensity of the laser beam exiting the measurement chamber can serve to diagnose optical misalignment or fouling, which would lead to a decrease in intensity, as well as interruption or failure of the laser.

3.2 Conceptual Design

3.2.1 Optical/Mechanical Design

Figure 8 shows a schematic of the Phase II instrument's optical/mechanical system. The major change compared to the Phase I breadboard involves the use of two separate optical collection systems (each containing a pair of lenses, an interference filter, and a PMT) for the hydrogen (612 nm) and water vapor (594 nm) channels. Except for the

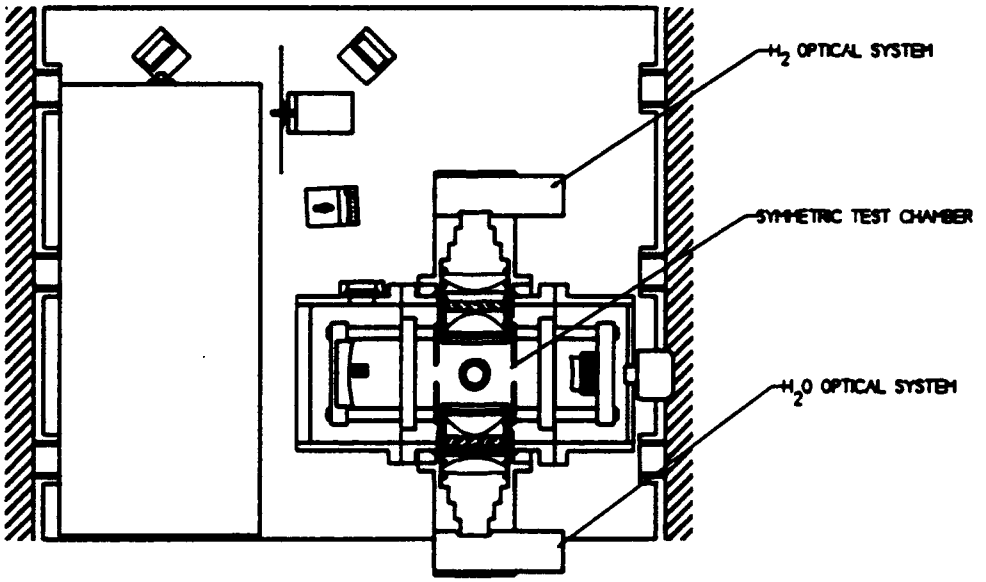

Figure 8. Conceptual Phase II RHS Sensor Design, Top Cross-Sectional View. The Layout is Similar to the Breadboard Instrument (Fig. 3), Except for the Addition of a Second Set of Collection Optics.

entrance window for the laser beam, the measurement chamber and the optical supports therein have mirror symmetry about the optical axis. Any thermal gradients generated by the incoming sample, which is introduced directly above the optical axis, will therefore cause no optical misalignment perpendicular to the symmetry plane. To further reduce thermal effects on alignment, critical mechanical components will be made of stainless steel, which has a smaller coefficient of expansion than aluminum, used in the Phase I components.

The laser will be a ~150 mW air-cooled argon ion laser similar in design to the Phase I laser, whose head dimensions are depicted in Fig. 8. The Phase II laser head would probably be bulkier, but not very much so; for example, Omnichrome's current 150 mW head is about 50% longer but of the same width. If a very compact instrument is desired, a diode-pumped doubled-YAG laser would be a suitable, although more expensive, alternative.

The measurement chamber will be electrically heated to just above 100° C to prevent condensation, and it would be thermally insulated from the remainder of the optical bench. To maintain the PMTs at near ambient temperature, the collection optics housings that support the PMTs will be made of a low thermal conductivity material. The PMTs will be cooled by a system fan which is also needed to cool the laser head.

The flow configuration in the chamber will be designed to minimize fouling of the optics by particulate or vapor contaminants in the sample. A "bottom outlet" design similar to that used in Phase I should prevent the buildup of contaminants in the chamber. Also, by extending the optical baffles beyond the rails, the inner volume between the baffles through which the sample flows can be isolated from the rest of the chamber. The air in front of the cavity mirrors will remain stagnant, protecting the mirrors from fouling. We anticipate that in normal use only the front surfaces of the collection lenses, which are close to the measurement region, will require periodic cleaning.

3.2.2 Electronics Design

The electronics will be basically similar to that of the Phase I breadboard and the hydrogen sensor developed by SSI for NASA/KSC.(2) The

electronics subassemblies consist of the laser controller, DC power supplies for the PMT and other electronic components, pressure gauge controller, signal processing circuitry, and I/O and diagnostic circuitry.

In the signal processing circuitry, the outputs from the PMT's will be appropriately buffered, scaled and subtracted, and then fed to the Evans Electronics lock-in board. As in the Phase I breadboard, the lock-in and pressure gauge outputs will be converted into a signal proportional to H_2 desired output voltage. The output amplifier will incorporate zero and span adjustments for calibrating the RHS to known gases.

The I/O and diagnostic circuitry will handle any desired remote interfacing and fault diagnostic functions. As described in Subsection 3.1.6, a threshold indicator on the exit beam photodiode output would trigger the fault diagnostic logic. In addition to the H_2 signal, other outputs may be of diagnostic value and could include the laser power and operating current as well as the system pressure and temperature readings.

3.2.3 Flow System Design

The flow system would be provided by AEDC; its design would be reviewed by both AEDC and SSI engineers to insure compatibility with the RHS instrument and rapid delivery of the air sample to it. Several implementations are possible. As originally proposed by SSI, and implemented in our Phase I tests, the sample would be drawn in by placing a mechanical pump downstream of the RHS; the exhausted gas would be vented to the outdoors. Alternatively, the pump could be placed upstream of the RHS and water separator. This would permit the RHS to be operated at atmospheric pressure, where its sensitivity is best. If the sample air cools sufficiently during its passage out of the duct, a standard bellows-type pump would be suitable. The internal volume of the pump would be too small to adversely affect the time response. On the contrary, faster transport down the sample line might result with this upstream pump configuration since the pressure drop would no longer be limited by the finite pressure in the duct.

3.2.4 Anticipated Performance

The anticipated performance of the Phase II brassboard RHS can be estimated by simply scaling the signal and noise levels from the Phase I breadboard. Assuming an 8-fold increase in laser power (150 mW in Phase II versus 18 mW in Phase I), and factors-of-two decrease in photon collection efficiency due to the elimination of the collection mirrors, the signal levels will be four times as large as in Phase I. In the low H_2 limit, this leads to a four-fold increase in the signal-to-noise ratio, to 40:1 or greater RMS at 1% H_2, P = 2 to 15 PSIA, or 20:1 at 1 PSIA.

In the high H_2 limit, the increased laser power leads to a two-fold increase in the signal-to-noise ratio compared to Phase I, since here the main noise source is shot noise, which increases with the square root of the signal. Thus, at 5% H_2 at 1 atm the noise-equivalent H_2 concentration will be 0.025%. While this is a larger absolute noise level than at lower H_2 concentrations, it is very small compared to the concentration itself. Thus, the actual measurement accuracy is not expected to be either detector- or shot-noise-limited at high concentrations, but will instead be limited by fluctuations in the laser or the electronics. The short-term stability of the laser and electronics should be such that relative measurements can be made with about 1% precision. Long-term drifts which tend to degrade the accuracy of absolute measurements will be designed to contribute no more than a 5% error.

Taking into account all of these sources of noise, we estimate the absolute measurement accuracy, including drift, to be within 5% of the H_2 concentration or 0.05%, whichever is larger, in the Phase II brassboard instrument at 1 PSIA. The accuracy will be considerably better at higher pressures, and the precision will also be improved in short-term measurements, where drift is not a factor.

4. SUMMARY AND CONCLUSIONS

The concept of using Raman scattering for rapid, sensitive and accurate detection of hydrogen concentrations in process air samples has been successfully demonstrated in Phase I of the RHS (Raman Hydrogen Sensor) development program, whose ultimate goal is to develop a practical hydrogen monitor for air samples from the engine test facility at AEDC. A laboratory breadboard instrument and gas handling manifold were built and tested in Phase I. The H_2 concentrations, gas temperatures, and total pressures were representative of the anticipated process air samples. The demonstrated detection limit for H_2 was 0.00013 atm using 18 mW of optical power from an air-cooled argon ion laser and an electronics integration time of 0.1 sec. The response time is a function of the inlet pipe size and the pumping speed; the fundamental response time of the Phase I instrument was found to be 0.3 sec using a 3/8" ID inlet pipe and a 3 ft^3/min pump rate. The effect of water vapor on the instrument output was characterized, and the feasibility of active subtraction of background water signals using a second optical channel was demonstrated. The performance of the instrument was in good agreement with theoretical calculations of the signal-to-noise ratio.

A conceptual design for a brassboard instrument to be built in Phase II has also been developed. Its optical design is similar to the proven Phase I design. The main goals will be to upgrade the optical system for better sensitivity and background rejection, to provide a heated measurement chamber, and to integrate the components into a rugged package for field testing. The results from the Phase I tests give us confidence that the Phase II instrument will meet or exceed the design goals for sensitivity, absolute accuracy, and sample compatibility.

5. REFERENCES

1. S. Adler-Golden, N. Goldstein, and F. Bien, U.S. Patent 4,953,976 (September 4, 1990).

2. S. M. Adler-Golden, F. Bien, W. K. Cheng, M. E. Gersh, M. W. Matthew, S. C. Richtsmeier, and N. Goldstein, "Hydrogen Laser Monitoring System (HLMS) Phase II Final Report," Spectral Sciences Inc. Rpt. No. SSI-TR-182. Prepared for John F. Kennedy Space Center under Contract No. NAS10-11514 (January 1991).

3. D. Herriott, H. Kogelnik, and R. Kompfner, "Off-Axis Paths in Spherical Mirror Interferometers," Appl. Opt., 3, 523-526 (1964).

4. W. R. Trutna and R. L. Byer, "Multi-Pass Raman Gain Cell," Appl. Opt., 19, 301-312 (1980).

5. S. M. Adler-Golden, N. Goldstein, F. Bien, M. W. Matthew, M. E. Gersh, W. K. Cheng, and F. W. Adams, "Laser Raman Sensor for Measurement of Trace-Hydrogen Gas," Appl. Opt., in press (1991).

6. J. A. Cooney, "Uses of Raman Scattering for Remote Sensing of Atmospheric Properties of Meteorological Significance," Opt. Eng., 22, 292-301 (1983).